ELSEVIER

Journal of Photochemistry and Photobiology A: Chemistry 91 (1995) 173–177

Journal of PHOTOCHEMISTRY AND PHOTOBIOLOGY A:CHEMISTRY

IR multiphoton absorption in Si_2F_6

V. Tosa [1], S. Isomura, K. Takeuchi

Institute of Physical and Chemical Research, Wako-shi, Saitama 351-01, Japan

Received 24 March 1995; accepted 24 May 1995

Abstract

IR multiphoton absorption (IRMPA) in neat Si_2F_6 was measured. The average number of photons absorbed per molecule and the absorption cross-sections are reported as a function of fluence for the 10R(12), 10R(22) and 10R(34) CO_2 laser lines. IRMPA spectra, given in the range from 10R(10) to 10R(38) for three different laser fluences, are discussed and compared with the multiphoton dissociation data.

Keywords: Hexafluorodisilane; Infrared multiphoton absorption; Absorption cross section; Frequency dependence; Fluence dependence

1. Introduction

IR multiphoton absorption (IRMPA) is the basis for understanding the processes taking place during and after the interaction of polyatomic molecules with high-intensity IR laser photon fields. In particular, the IR multiphoton decomposition (IRMPD) of polyatomic molecules will be essentially dependent on the IRMPA characteristics. Although detailed IRMPA studies have been performed for many individual molecules, to our knowledge, no such studies have been reported for hexafluorodisilane (Si_2F_6), a symmetric top molecule of interest in Si film deposition and Si isotope separation technologies.

The pulsed radiation of a CO_2 laser induces efficient IRMPA in the $\nu_7 = 992\ cm^{-1}$ [1] normal mode of Si_2F_6. The subsequent IRMPD has been investigated both as a potential method for Si isotope separation [2,3] and as the most efficient way of generating the SiF_2 long-lived radical [4,5]. Laser isotope separation of ^{29}Si and ^{30}Si by IRMPD of gaseous Si_2F_6 has been investigated by Arai and coworkers [2,3]. Their parametric study [3] reported the yield of SiF_4 formation in the MPD of Si_2F_6 and its dependence on the gas pressure, laser excitation frequency and laser fluence. The formation of the SiF_2 radical in the IRMPD of Si_2F_6 and the reactions of SiF_2 with Br_2, NO_2 and C_2H_4 have been investigated recently [5] by time-resolved IR diode laser spectroscopy. The simultaneous formation of SiF_4 and SiF_2 confirms that the reaction $Si_2F_6 \rightarrow SiF_4 + SiF_2$ is the main channel for dissociation.

Our study on the vibrational spectroscopy of this molecule [1] yielded improved values for the normal mode frequencies and the force field constants. The measurement of the Raman active $2\nu_4 \leftarrow 0$ transition allowed us to estimate the torsional frequency $\nu_4 = 38\ cm^{-1}$ and the barrier to the internal rotation $V_3 = 510–550\ cm^{-1}$. Recently, we also reported the high-resolution ν_5 parallel bands [6] and the ν_7 perpendicular bands [7] for the major isotopomers of Si_2F_6 cooled in a supersonic free jet. These studies provided valuable information for the understanding of IRMPA: band origins, rotational constants, isotopic shifts and Coriolis constants.

In this paper, we report the IRMPA characteristics of gaseous Si_2F_6 in pulsed CO_2 laser photon fields. For the 10R(10) to 10R(38) range of laser lines, we measured the number of photons absorbed per molecule and the average IRMPA cross- sections as a function of laser fluence. The IRMPA spectra, i.e. the number of photons absorbed as a function of laser frequency, are reported for three different laser fluences. The dependence of the IRMPA parameters on the laser fluence for individual laser lines is illustrated here only for the 10R(12), 10R(22) and 10R(34) CO_2 laser lines, which are representative of the IRMPA process in Si_2F_6. The present IRMPA data have been correlated with the available spectroscopic and MPD data and a better understanding of the Si_2F_6 interaction with pulsed IR radiation has been obtained.

2. Experimental details

For the hexafluorodisilane preparation, Si_2Cl_6 should be obtained first. Ferrosilicon (60% Si, 40% Fe) was mixed with 2 wt.% of potassium chloride as catalyst. The mixture

[1] On leave from the Institute of Isotopic and Molecular Technology, Cluj-Napoca, Romania.

1010-6030/95/$09.50 © 1995 Elsevier Science S.A. All rights reserved
SSDI 1010-6030(95)04126-5

was maintained at about 160 °C and chlorine gas was passed slowly through the reaction tube. The product contained about 50% of Si_2Cl_6 and was separated by fractional distillation.

Hexafluorodisilane was prepared by gently warming together Si_2Cl_6 (6 g), anhydrous antimony fluoride SbF_3 (25 g) and a small amount of $SbCl_5$ (1 ml) as catalyst; thus

$$Si_2Cl_6 + 2SbF_3 \longrightarrow Si_2F_6 + 2SbCl_3$$

The product was collected in a small glass bulb, and a low-temperature distillation was carried out by the bulb to bulb method at −90 °C. The final purity of Si_2F_6 (as checked by gas chromatography and Fourier transform IR (FTIR) spectroscopy) was about 98%, the main impurity being SiF_4.

The IRMPA measurements were performed with a Lumonics 103 CO_2 TEA laser operated at 0.3 Hz using an He–CO_2–N_2 mixture of 6 : 1 : 1. The unfocused beam was truncated by a 12.4 mm diameter iris and was attenuated by different combinations of CaF_2 flats. The Si_2F_6 gas was contained in a cross-shaped cell equipped with four KBr windows. The long arm (80 cm) of the cell was illuminated by the CO_2 pulsed radiation and the short arm (10 cm) was used to control the gas dissociation by recording the FTIR spectra before and after the experiment. A conventional vacuum line (MKS Baratron controlled) was used to fill and evacuate the cell down to 10^{-5} Torr since the gas was extremely moisture sensitive. The beam was split into two parts by a CaF_2 window. The small part of the beam was monitored by a pyroelectric detector to check the pulse energy during the measurements. A second calibrated Gentec pyroelectric detector measured, for each fluence value, the pulse energy of the main beam both in front of and behind the cell. The absorption in the cell windows (the empty cell) was measured for eight laser lines distributed over the entire range and the average absorbance of the empty cell was estimated. The energy values (one value being the average of 20 pulses), measured with empty (E_e) and filled (E_f) cells, were used to calculate the energy absorbed ($E_{abs} = E_e - E_f$) and the average number of photons ($\langle\langle n\rangle\rangle = E_{abs}/(Nh\nu)$) absorbed by the N Si_2F_6 molecules found in the interaction volume. The absorption cross-sections were calculated using $\langle\langle n\rangle\rangle(\Phi) = \sigma(\Phi)\Phi$ as in Ref. [8] or the formula $\sigma = -\ln(T)/nl$ where n is the molecular density. The two values were found to be identical within experimental error for the entire range of fluences used in the experiments.

During the measurements, we carefully checked the influence of dissociation on the absorption data. For one laser line, the cell was filled once with 0.1 Torr of gas and the absorption was measured for increasing values Φ_0, Φ_1, Φ_2,... of laser fluence. After obtaining the data for one fixed fluence Φ_k, we measured the absorption again for the lowest fluence Φ_0, and compared it with the absorption obtained initially for the same Φ_0. As the two (average) values will be proportional to the number of absorbing molecules in the interaction volume, we used their ratio to multiply the absorption data for Φ_k, hence compensating for the influence of dissociation. As a rule, we limited the laser fluence to low values so that the correction was applied only to the highest fluence points of the most absorbing lines, the rest of the data being, within experimental error, unaffected by dissociation.

The measurement of the average absorption cross-sections must involve optically thin cells. As demonstrated in Ref. [9], in IRMPA experiments, the absorption cells can be regarded as optically thin within 2% error even if as much as 40% of the incident energy is absorbed. In our experiments, the energy absorbed by Si_2F_6 ranged from 5% to 35% of the total incident energy, so that we applied no correction for the intensity of the laser beam within the absorption cell.

3. Results and discussion

The present data refer to a constant pressure of 0.1 Torr of neat Si_2F_6. For comparison purposes, we represented the number of photons absorbed as a function of the normalized fluence $\sigma_0\Phi$, where σ_0 is the spectroscopic absorption cross-section. Since, in the low-fluence region, we must have, to a fairly good approximation, a constant cross- section, we calculated σ_0 as

$$\sigma_0 = \left.\frac{d\langle\langle n\rangle\rangle}{d\Phi}\right|_{\Phi\to 0}$$

In practice, we performed a linear least-squares fit of the lowest fluence absorption data and calculated $\sigma_0(\nu)$ for all laser lines. The average cross-sections obtained in this way are represented in Fig. 1, together with the values $\sigma_0(\nu)$ derived from the FTIR spectrum of the ν_7 band. As the agreement between the two sets of data is fairly good, in the cal-

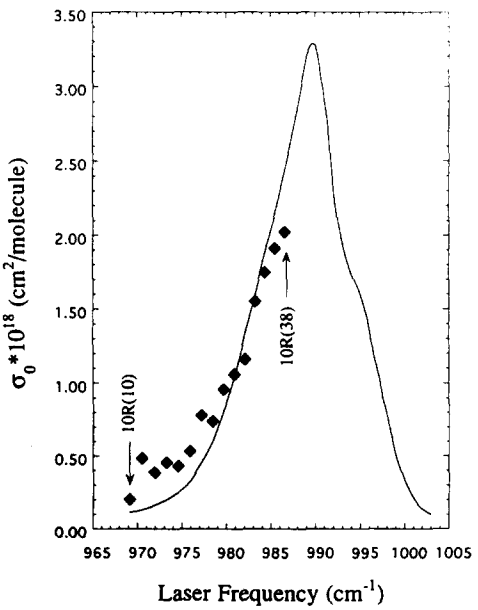

Fig. 1. Spectroscopic cross-section σ_0 as obtained from the ν_7 FTIR spectrum of Si_2F_6 (cell length, 10 cm; 0.1 Torr) at 2 cm^{-1} resolution. The points represent the σ_0 values obtained as described in the text for the CO_2 laser frequencies used in the IRMPA measurements.

culation of $\sigma_0\Phi$, we used the σ_0 values derived from the IRMPA experiments.

The plots of $\langle\langle n\rangle\rangle$ as a function of $\sigma_0\Phi$ are shown in Fig. 2 for the 10R(12), 10R(22) and 10R(34) lines. The low-fluence data for the three laser lines group around the same line with a slope of unity; however, there are also deviations from this line. For the 10R(12) line, positive deviations from the linearity of $\langle\langle n\rangle\rangle$ vs. $\sigma_0\Phi$ can be noted as the fluence increases. A possible explanation is that, at high fluences, absorption takes place through direct n-photon resonance processes, namely through processes in which a molecule absorbs resonantly n photons. In such a process $\langle\langle n\rangle\rangle \propto \Phi^n$; however, in an ensemble of molecules, only a small fraction will undergo this resonant absorption, namely those initially found in favourable vibrational-rotational states. As a result, the macroscopic effect observed is only a slight deviation from a linear dependence. It should be noted that this stronger than linear dependence of $\langle\langle n\rangle\rangle$ on $\sigma_0\Phi$ was observed for all the laser lines red shifted from the ν_7 absorption maximum, but the deviation decreased continuously as the laser frequency increased towards the ν_7 maximum.

As revealed by experiments on many polyatomic molecules [10], when the excitation frequency is close to the normal mode frequency, the fluence dependence of $\langle\langle n\rangle\rangle$ can be written as

$$\langle\langle n\rangle\rangle \propto \Phi^{\gamma}$$

where the power index γ takes two limiting values: (1) for low laser fluences, $\gamma \approx 1$, thus a linear dependence is observed; (2) as the fluence increases, the power index tends to the limiting value $\gamma \approx 2/3$. The type of dependence corresponds to $\sigma_0\Phi/q > 1$ (case 2) or $\sigma_0\Phi/q < 1$ (case 1), where q is the fraction of excited molecules.

The above rule has been shown in our case for the laser lines close to the ν_7 frequency (see Fig. 1). As an example, we have chosen the data for the 10R(34) line (Fig. 2). We can see that the low-fluence points align on the line with a slope of unity, whereas a least-squares fit of the high-fluence data yields a slope of 0.62 in the log–log plot. The transition from the $\gamma = 1$ to $\gamma = 2/3$ regime takes place gradually as the fluence increases; it is observed around 0.01 J cm^{-2}.

The average absorption cross-sections as a function of laser fluence, presented in Fig. 3, coincide with the dependence of $\langle\langle n\rangle\rangle$ on $\sigma_0\Phi$. In particular, a constant cross-section corresponds to a linear dependence of $\langle\langle n\rangle\rangle$ on $\sigma_0\Phi$, whereas the increase in cross-section for the 10R(12) line corresponds to positive deviations from linearity. At the same time, the $\langle\langle n\rangle\rangle \propto (\sigma_0\Phi)^{2/3}$ dependence corresponds to the $\sigma \propto \Phi^{-1/3}$ power law [10] which is again exemplified in Fig. 3 with the 10R(34) data. The same dependence has been found by our group for UF_6 [11] in the case of an excitation frequency slightly red shifted with respect to its ν_3 fundamental.

The data presented above for the three laser frequencies demonstrate that the same molecule can behave quite differently for different excitation wavelengths.

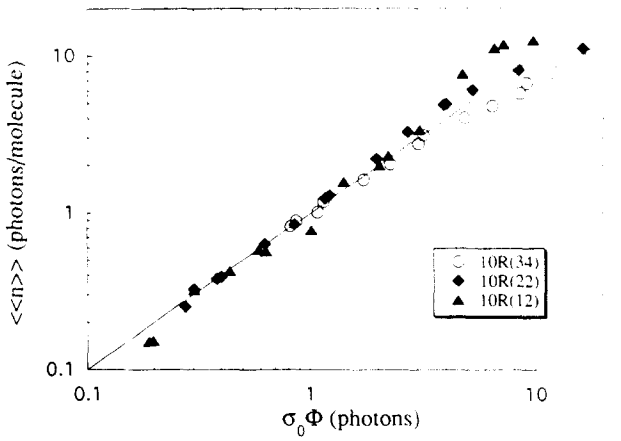

Fig. 2. Number of photons absorbed as a function of the normalized fluence $\sigma_0\Phi$ for the laser lines indicated on the graph. The line has been drawn with a nominal slope of unity (see text for details).

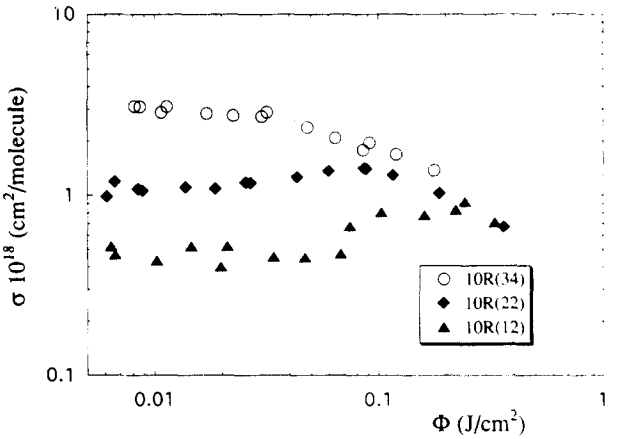

Fig. 3. Si_2F_6 average IRMPA cross-sections as a function of the laser fluence Φ for the same laser lines as in Fig. 2.

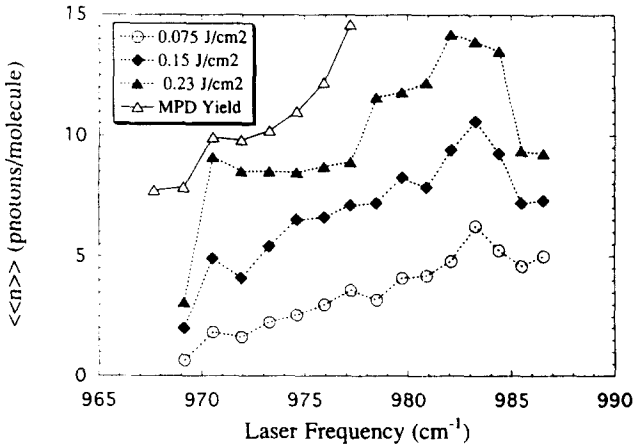

Fig. 4. IRMPA spectra of Si_2F_6 for three different laser fluences. The MPD yield data of Ref. [2] are also given in arbitrary units for comparison.

Finally, we present in Fig. 4 the average number of photons absorbed per molecule as a function of the laser frequency for the following laser fluences: 0.075, 0.15 and 0.23 J cm^{-2}. The spectra were obtained using the $\langle\langle n\rangle\rangle = \langle\langle n\rangle\rangle(\Phi)$ data points for an interpolation around these fluences. We can

outline some interesting features of the IRMPA spectra presented in Fig. 4. Firstly, the IRMPA maximum is, in all three cases, around 983 cm^{-1}, which is red shifted by about 7 cm^{-1} from the ν_7 band maximum (see Fig. 1). As expected, the mode anharmonicity induces an increase in this shift as the laser fluence increases. Secondly, there is a strong decrease in IRMPA for laser lines below 970 cm^{-1}; however, as the laser fluence increases, the absorption for these lines becomes significant and a new local maximum appears around 970 cm^{-1}.

It is interesting to compare the IRMPA spectrum obtained for 0.23 J cm^{-2} and 0.1 Torr of Si_2F_6 with the MPD data reported in Ref. [2] for 0.25 J cm^{-2} and 2 Torr gas pressure. For this reason Y_{28}, the relative yield of $^{28}SiF_4$, is also represented in Fig. 4. As can be seen, the two sets of data follow the same trend: both the number of photons absorbed and the MPD yield of SiF_4 exhibit a considerable increase for laser frequencies greater than 970 cm^{-1}. In addition, the local IRMPA maximum observed in the absorption for the 10R(12) line is observed in Ref. [2] for the same line. In explaining this local maximum, we could assume that the leftmost part of the spectrum is influenced by the isotopic species present in the sample. However, this assumption must be discarded for the following reasons. The major isotopic species $^{28,28}Si_2F_6$ (85.1%) and $^{28,29}Si_2F_6$ (8.6%) have their band origins at 992.3 and 988.4 cm^{-1} [7]; hence we should also expect a shift of about 4 cm^{-1} between the successive IRMPA maxima of different isotopic species. If the maximum at 983 cm^{-1} is assigned to $^{28,28}Si_2F_6$, then around 971 cm^{-1} we should find the maximum of $^{29,30}Si_2F_6$. However, this species can contribute to the absorption according to its natural abundance (0.29%), a contribution which would be barely noticeable in Fig. 4. Furthermore, the leftmost peak at 970 cm^{-1} is reproduced by the maximum in the dissociation yield of the abundant isotope.

A more plausible explanation for the origin of the maxima observed in the IRMPA spectra in Fig. 4 is that direct multiphoton transitions take place in the molecule and enhance the IRMPA process. The frequency of such resonances will depend mainly on the structure of the higher vibrational levels of the ν_7 ladder, but the parameters characterizing this structure are unknown. However, the anharmonicity constant of the ν_7 ladder can be estimated roughly by the formula [12]

$$X_{77} = \frac{\nu_7^2}{4D_{Si-F}}$$

where D_{Si-F} is the dissociation energy of the Si–F bond. We find $X_{77} = 3$ cm^{-1} (for $D_{Si-F} = 139$ kcal mol^{-1} [13]) and $X_{77} = 5$ cm^{-1} (for $D_{Si-F} = 222$ kcal mol^{-1} [14]). For the simple anharmonic oscillator approximation and neglecting the rotational structure, the frequency of an n-photon resonance is shifted with respect to the fundamental by nX_{77}, which means that in the region around 983 cm^{-1} we have the frequency of two- or three-photon resonances. This result is highly simplified, however, it supports the assumption about the presence of multiphoton resonances in our spectra. Two- and three-photon resonances have also been observed in the IRMPA spectra of other polyatomic molecules (for a review, see Ref. [15]).

The above arguments advance the idea that, at least in the ν_7 mode, the anharmonicities are large. On the other hand, the small change in σ with Φ (see Fig. 3) points to a small anharmonicity. To our knowledge, the only mechanism proposed to explain a nearly linear absorption in spite of a large anharmonicity is the cooperation between rotational compensation and anharmonic splitting, advanced by Fuss and Kompa [16] and developed for symmetric tops. For Si_2F_6, the distribution of molecules on the rotational levels of the initial vibrational levels is particularly broad: for example, the maximum of this distribution for the ground state is around $J = 60$. In the ν_7 ladder of states, we have the usual $\Delta n = \pm 1$ and $\Delta J = 0, \pm 1$ transition rules; only $\Delta K = \pm 1$ transitions are allowed for the ν_7 fundamental; however, for higher vibrational states, both $\Delta K = \pm 1$ and $\Delta K = 0$ are allowed. In these conditions, the total number of states involved in the multiphoton process rapidly increases with n, and the rotational compensation of the anharmonicity is expected to play a central role. Anharmonic and Coriolis splittings are also expected to generate additional paths for excitation and thus to enhance the overall absorption cross-sections.

At this point we should stress another important fact: in our experimental conditions (static cell, room temperature), the IRMPA process in Si_2F_6 results from many contributions. The low-frequency normal modes $\nu_9 = 153$, $\nu_{12} = 202$ and $\nu_3 = 218$ cm^{-1} and, especially, the torsional mode at $\nu_4 = 38$ cm^{-1} will generate many low-lying vibrational-torsional levels with significant populations. A simple calculation shows that, at room temperature, the ground state population is 0.40%, while the ν_4, ν_9, ν_{12} and ν_3 populations are 0.34%, 0.16%, 0.14% and 0.12% respectively. Hot-band multiphoton transitions, such as $\nu_4 \rightarrow \nu_4 + \nu_7 \rightarrow \nu_4 + 2\nu_7 \rightarrow \ldots$ have a sizeable contribution to the observed absorption; thus it is reasonable to assume that the red shift observed is partly due to these hot-band transitions. It should be noted that the hot-band contribution is clearly present in the ν_7 spectrum: the maximum of the band (see Fig. 1) is at 990 cm^{-1}, while the most prominent peak of jet-cooled Si_2F_6 is $^RQ_0$ at 992.3 cm^{-1} [7]. A computer calculation of the ν_7 band profile at 300 K, neglecting the hot-band contributions, yields a maximum at 992.2 cm^{-1}.

4. Conclusions

To summarize, we have performed a study of the IRMPA in Si_2F_6. The number of photons absorbed per molecule and the average cross-sections were measured in this spectral region. The general behaviour, valid for many polyatomic molecules, has also been found for Si_2F_6, as far as the IRMPA dependence on the laser fluence is concerned. The depend-

ence on the laser frequency reveals a large anharmonic shift in the IRMPA maxima, which is a combined effect of the ν_7 mode anharmonicity and the hot- band contributions to the absorption. A close correlation between the IRMPA and previous MPD spectra has been found and a better understanding of these two processes has been obtained.

References

[1] V. Tosa, S. Isomura, Y. Kuga and K. Takeuchi, *Vib. Spectrosc., 8* (1994) 45.

[2] S. Arai, H. Kaetsu and S. Isomura, *Appl. Phys. B, 53* (1991) 199.

[3] M. Kamioka, Y. Ishikawa, H. Kaetsu, S. Isomura and S. Arai, *J. Phys. Chem., 90* (1986) 5727.

[4] F.W. Lampe and J. Biedrzycki, *Spectrochim. Acta, Part A, 46* (1990) 631.

[5] K. Sugawara, F. Ito, T. Nakanaga and H. Takeo, *Chem. Phys. Lett., 232* (1995) 561.

[6] R.-D. Urban, V. Tosa, M. Takami and K. Takeuchi, *J. Mol. Spectrosc., 170* (1995) 42.

[7] V. Tosa, R.-D. Urban, M. Takami and K. Takeuchi, *J. Mol. Spectrosc., 172* (1995) 254.

[8] O.P. Judd, *J. Chem. Phys., 71* (1979) 4515.

[9] M.T. Duignan, D. Garcia and E. Grunwald, *J. Am. Chem. Soc., 103* (1981) 7281

[10] See, for example, J.L. Lyman, G.P. Quigley and O.P. Judd, in C.D. Cantrell (ed.), *Topics in Current Physics*, Vol. 35, Springer, Berlin, 1986.

[11] Y. Okada, H. Tashiro and K. Takeuchi, *J. Nucl. Sci. Technol., 30* (1993) 762.

[12] G. Herzberg, *Spectra of Diatomic Molecules*, Van Nostrand, New York, 2nd edn., 1950, p. 100.

[13] P. Ho and C.F. Melius, *J. Phys. Chem., 94* (1990) 5120.

[14] J.D. McDonald, C.H. Williams, J.C. Thompson and J.L. Malgrave, *Adv. Chem. Ser., 72* (1968) 261.

[15] V.N. Bagratashvili, V.S. Letokhov, A.A. Makarov and E.A. Ryabov, *Multiple Photon Infrared Laser Photophysics and Photochemistry*, Harwood Academic Publishers, New York, 1985.

[16] W. Fuss and K.L. Kompa, *Prog. Quantum Electron, 7* (1981) 117.